

Enhancing parameter estimation in finite mixture of generalized normal distributions

Pierdomenico Dutillo^{1,*}, Stefano Antonio Gattone²

¹*Department of Statistical Sciences, University of Padova, Padova, Italy*

²*DiSEGS, University "G. d'Annunzio" of Chieti-Pescara, Pescara, Italy*

*Corresponding author: pierdomenico.dutillo@unipd.it

Abstract

Mixtures of generalized normal distributions (MGND) have gained popularity for modelling datasets with complex statistical behaviours. However, the estimation of the shape parameter within the maximum likelihood framework is quite complex, presenting the risk of numerical and degeneracy issues. This study introduced an expectation conditional maximization algorithm that includes an adaptive step size function within Newton-Raphson updates of the shape parameter and a modified criterion for stopping the EM iterations. Through extensive simulations, the effectiveness of the proposed algorithm in overcoming the limitations of existing approaches, especially in scenarios with high shape parameter values, high parameters overall and low sample sizes, is shown. A detailed comparative analysis with a mixture of normals and Student-t distributions revealed that the MGND model exhibited superior goodness-of-fit performance when used to fit the density of the returns of 50 stocks belonging to the Euro Stoxx index.

Keywords: mixture of generalized normal distribution, spurious solutions, ECM algorithm, adaptive step size

1 Introduction

Over time, non-normal mixture distributions have gained increasing attention for modelling random variables with leptokurtic, heavy-tailed, and skewed distributions (Lee and McLachlan, 2013). Among the statistical distributions available in the literature, the generalized normal distribution (GND) is capable of describing a large variety of statistical behaviours due to the additional shape parameter that controls the weight of the tails. (Nadarajah, 2005). The GND is a natural generalization of the normal distribution, also known as the generalized Gaussian distribution, exponential power distribution, or generalized error distribution. Nadarajah (2005) initially examined the statistical characteristics of the GND, including the hazard rate function, moments, and maximum likelihood estimation, while Pogány and Nadarajah (2010) focused on the characteristic function of the GND.

Mixtures of generalized normal distribution (MGND) have attracted considerable interest due to their flexibility to model complex data, including applications in image processing

(Bazi et al., 2006; Allili et al., 2008) and speech modelling (Kokkinakis and Nandi, 2005; Deledalle et al., 2018). Estimation of parameters is performed using the maximum likelihood estimation (MLE) and the expectation-maximization (EM) algorithm (Dempster et al., 1977). Since the system to resolve the updating equation of the mean and the shape parameters is heavily nonlinear, the numerical optimization based on the Newton-Raphson method is used. However, the Newton-Raphson update of the shape parameter becomes challenging, especially when its value is greater than 2, causing the algorithm to diverge and produce incorrect values (Roenko et al., 2014; Deledalle et al., 2018). For example, in the case of the GND distribution, some studies (Kokkinakis and Nandi, 2005; Krupiński and Purczyński, 2006; Roenko et al., 2014; Deledalle et al., 2018) limit the shape parameter to a range of 0.3-2. As an alternative, Nguyen et al. (2014) proposed a univariate bounded generalised Gaussian mixture model defining a bounded support region in \mathbb{R} for each component of the mixture. Mohamed and Jaïdane-Saïdane (2009) estimated the shape parameter using the analytical relationship between the shape parameter and kurtosis, while moment-matching and entropy-matching estimators have been proposed by Roenko et al. (2014) and Kokkinakis and Nandi (2005), respectively. Even if these estimators have the advantage of relative simplicity, they are less accurate than MLE.

Recently, Wen et al. (2022) studied the statistical properties of a two-component MGND and performed MLE using an expectation conditional maximization (ECM) algorithm. The ECM algorithm (Meng and Rubin, 1993) is an extension of the EM algorithm which adjusts the M-step into several conditional maximization steps. Wen et al. (2022) emphasised the need to improve the convergence rate of parameter estimation, suggesting the Regula-Falsi iteration method (Roenko et al., 2014) as a potential solution.

The present work aims to enhance MGND maximum likelihood estimation by including an adaptive step size function for the Newton-Raphson update of the shape parameter and a different stopping criterion for the EM iterations (Algorithm 2 in Appendix D). The proposed algorithm is denoted as ECMs (expectation conditional maximization with step size).

The numerical and degeneracy issues we try to address are illustrated by the following motivating example. Using algorithm 3 in Appendix D, we simulated a sample of $N = 250$ observations from a two-component MGND model with mixture weights $\pi_1 = 0.7$ and $\pi_2 = 0.3$, location parameters $\mu_1 = 1$ and $\mu_2 = 5$, scale parameters $\sigma_1 = 3$ and $\sigma_2 = 1$, and shape parameters $\nu_1 = 5$ and $\nu_2 = 1.5$. Table 1 reports the log-likelihood and the parameter estimates obtained by applying the plain ECM and the proposed ECMs algorithms together with the estimated variance and kurtosis. Figure 1 shows the convergence of the parameters estimation. With the ECM algorithm, the likelihood function is maximized after 40 iterations, but the final solution is a spurious solution: the degeneracy of $\hat{\nu}_1 = 14.8716$ from its real value $\nu_1 = 5$ is remarkable. On the other hand, the proposed ECMs algorithm avoids the degeneracy of the shape parameter whereas $\hat{\nu}_1 = 5.1572$, very close to the true value of the parameter. In this example, the degeneracy of ν_1 contributes to worsening the estimates of the other parameters. Figure 2 reports the mixture and component densities estimates obtained with the two algorithms. The ECM algorithm provides a very poor

recovery of the single components while obtaining a reasonable estimate of the marginal distribution. However, the fit obtained using the ECMs algorithm is largely improved.

Table 1: Parameter estimates of the ECM and ECMs algorithms (motivating example).

	π_1	μ_1	σ_1	ν_1	π_2	μ_2	σ_2	ν_2	VAR(X)	Kur(X)	$\log L(\theta)$
	0.7	1	3	5	0.3	5	1	1.5			
ECM	0.5972	0.4100	2.6871	14.8716	0.4028	4.589	1.6428	2.4471	6.0240	1.4011	-551.0531
ECMs	0.6933	0.9149	2.9680	5.1572	0.3067	4.9765	1.1239	1.6666	5.7232	1.4537	-551.7986

Notes. The sample variance and kurtosis are equal to 5.7785 and 1.8966, respectively.

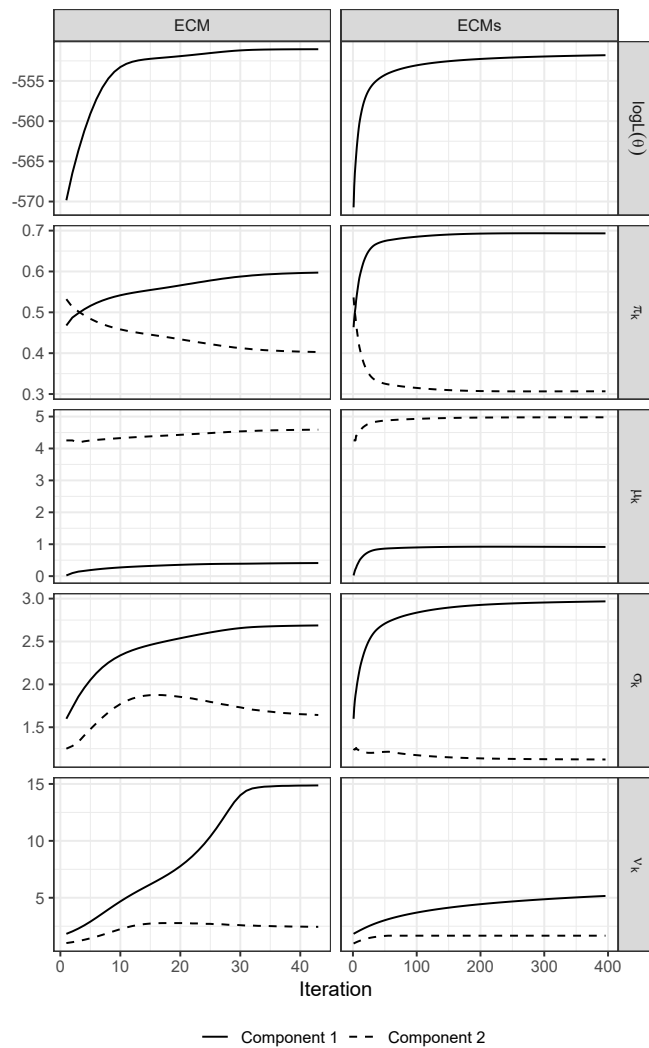


Figure 1: Convergence of parameter estimates (motivating example).

The poor performance of the ECM algorithm is related to some specific features of the MGND model. From Figure 3, we can observe how the variance, the kurtosis, and the log-likelihood of the MGND model in Table 1 change as a function of the shape parameters ν_1 and ν_2 , keeping all other parameters fixed. Variance and kurtosis decrease as shape

parameters increase but they tend to stabilize over values of ν greater than 2. In addition, the nearly flat log-likelihood surface that arises when $\nu > 2$ (Figure 3) makes it difficult to find sensible estimates, as many values of ν are fairly equally likely.

Two insights are gained from the motivating example. First, an EM stopping criterion based on the difference of the likelihood value (or the MGND parameters) may not always be a good indicator for stopping the algorithm. Second, a smaller step size could be used in the Newton-Raphson update to prevent the degeneracy of the shape parameter. In fact, Dutillo (2024) proposed including a step size in the Newton-Raphson update. However, an open issue was the choice of an appropriate value that could vary according to different scenarios.

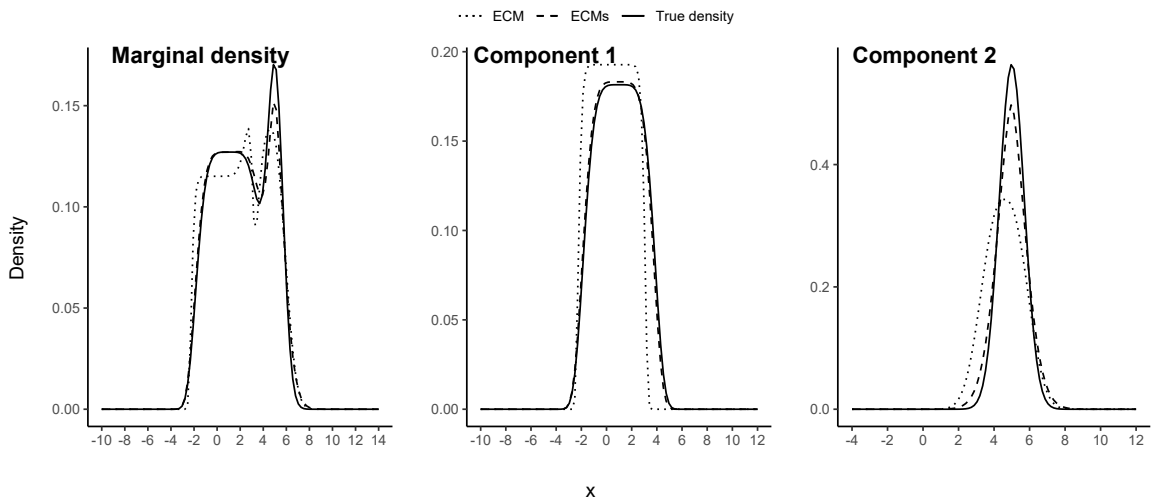


Figure 2: Motivating example - estimated densities.

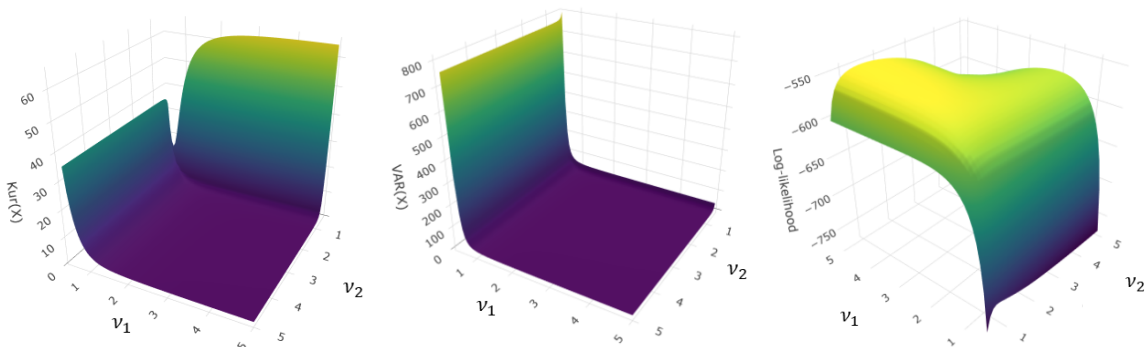


Figure 3: Motivating example - functional relationships and log-likelihood surface.

The rest of the paper is organised as follows. Statistical properties and central moments of the finite mixture of univariate generalized normal distribution are presented in Section 2. The proposed ECMs algorithm for maximum likelihood estimation (MLE) of the MGND model is presented in Section 3 and its performance is evaluated under different simulated

scenarios in Section 4. An empirical application is presented in Section 5 where the goodness of fit of the two-component MGND model is compared to that of two well-known competing methods: the two-component mixture of normals (MND) and the two-component mixture of Student-t distributions (MSTD). Finally, Section 6 provides some conclusions.

2 Mixture of generalized normal distribution

A random variable X is said to have the GND with location μ , scale σ and shape ν if its pdf is given by

$$f_{GND}(x|\mu, \sigma, \nu) = \frac{\nu}{2\sigma\Gamma(1/\nu)} \exp\left\{-\left|\frac{x-\mu}{\sigma}\right|^\nu\right\}, \quad (1)$$

with $-\infty < x < \infty$, $-\infty < \mu < \infty$, $\sigma > 0$, $\nu > 0$, $\Gamma(t) = \int_0^\infty x^{t-1} \exp(-x) dx$ for $t > 0$.

Figure 4 shows the probability density function of the GND (Eq. 1) for $\mu = 1$, $\sigma = 1$ and different shape values. The shape parameter ν controls both the peakedness and the tail weights. If $\nu = 1$ the GND reduces to the Laplace distribution and if $\nu = 2$ it coincides with the normal distribution. It is noticed that $1 < \nu < 2$ yields an “intermediate distribution” between the normal and the Laplace distribution. As limit cases, for $\nu \rightarrow \infty$ the distribution tends to a uniform distribution, while for $\nu \rightarrow 0$ it will be impulsive (Nadarajah, 2005; Bazi et al., 2006; Dytso et al., 2018).

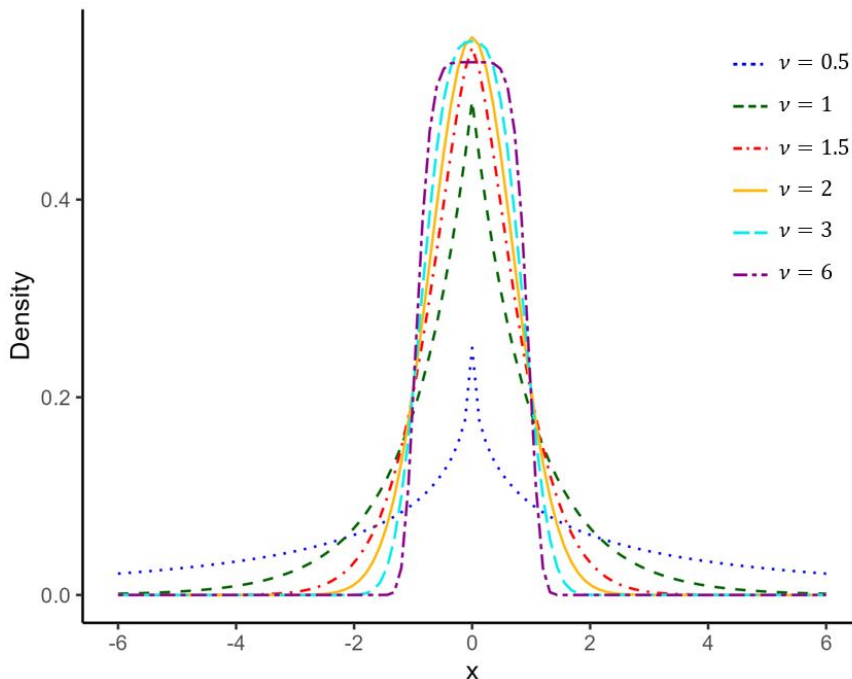


Figure 4: GND densities for $\mu = 0$, $\sigma = 1$ and different shape values.

The n -th central moments, skewness, and kurtosis of the GND are reported in the Appendix (A). Varanasi and Aazhang (1989) and Nadarajah (2005) explored two methods for parameter estimation: the method of moments and the MLE. In any case, the estimates do

not have a closed form and must be obtained numerically by applying the Newton-Raphson method or the Nelder-Mead approach (Nelder and Mead, 1965).

A finite mixture of univariate generalized normal distributions (MGND) with K components is given by the marginal distribution of the random variable X

$$f_{MGND}(x|\theta) = \sum_{k=1}^K \pi_k f_k(x|\mu_k, \sigma_k, \nu_k), \quad (2)$$

where f_k is the density f_{GND} of the k -th component and $-\infty < x < \infty$. The set of all the mixture parameters is given by $\theta = \{\pi_k, \mu_k, \sigma_k, \nu_k, k = 1, \dots, K\}$ belonging to the parameter space $\Theta = \{\theta : 0 < \pi_k < 1, \sum_{k=1}^K \pi_k = 1, -\infty < \mu_k < \infty, \sigma_k > 0, \nu_k > 0, k = 1, \dots, K\}$ with $\dim(\theta) = p$. The two-component MGND ($K = 2$) is given by

$$f_{MGND}(x|\theta) = \pi_1 f_1(x|\mu_1, \sigma_1, \nu_1) + \pi_2 f_2(x|\mu_2, \sigma_2, \nu_2), \quad \text{with } \dim(\theta) = 7. \quad (3)$$

This model nests several distributions as its sub-models, namely according to the shape parameter value ν_k . For instance, equation 3 reduces to:

- Normal mixture model for $\nu_1 = \nu_2 = 2$;
- Laplace mixture model for $\nu_1 = \nu_2 = 1$;
- Normal-Laplace mixture model for $\nu_1 = 2$ and $\nu_2 = 1$;
- Normal-GND mixture model for $\nu_1 = 2$ and $\nu_2 > 0$;
- Laplace-GND mixture model for $\nu_1 = 1$ and $\nu_2 > 0$.

Looking at the n -th central moments, the skewness and kurtosis of the MGND reported in the appendix (B), it is clear that these quantities depend on all the parameters of the mixture and, as already seen in Figure 3, variance and kurtosis decrease as ν_1 and ν_2 increase.

3 The ECMs algorithm

In this section, we modify the ECM algorithm for parameter estimation of the MGND model (Bazi et al., 2006; Wen et al., 2022) by introducing an adaptive step size function for the Newton-Raphson update of the shape parameter and by modifying the standard EM stopping criterion based on the difference of the likelihood value.

A complete description of the ECM algorithm and the proposed ECMs algorithm is provided in Algorithm 1 and Algorithm 2 of Appendix D, respectively.

From equation 3 the log-likelihood function is given by

$$\log L(\theta) = \sum_{n=1}^N \log \left[\sum_{k=1}^K \pi_k f_k(x_n|\mu_k, \sigma_k, \nu_k) \right]. \quad (4)$$

The **E-step** involves computing the Q-function

$$Q(\theta, \theta^{(m-1)}) = \sum_{k=1}^K \sum_{n=1}^N z_{nk}^{(m-1)} \log \left[\pi_k^{(m-1)} f_k(x_n|\mu_k^{(m-1)}, \sigma_k^{(m-1)}, \nu_k^{(m-1)}) \right], \quad (5)$$

where

$$z_{nk}^{(m-1)} = \frac{\pi_k^{(m-1)} f_k(x_n | \mu_k^{(m-1)}, \sigma_k^{(m-1)}, \nu_k^{(m-1)})}{\sum_{k=1}^K \pi_k^{(m-1)} f_k(x_n | \mu_k^{(m-1)}, \sigma_k^{(m-1)}, \nu_k^{(m-1)})}. \quad (6)$$

The term $z_{nk}^{(m-1)}$ represents the current estimate of the posterior probability in the $m - 1$ -th iteration, that is, the probability that the observation n belongs to the group k given the parameters of the current component $\theta^{(m-1)}$.

The conditional **M-Step** maximizes the Q-function computed in equation (5) over θ so to increase the log-likelihood function in equation 4.

Mixture weights Set $\frac{\partial Q(\theta, \theta^{(m-1)})}{\partial \pi_k} = 0$, then

$$\pi_k^{(m)} = \frac{\sum_{n=1}^N z_{kn}^{(m-1)}}{\sum_{k=1}^K \sum_{n=1}^N z_{kn}^{(m-1)}}. \quad (7)$$

Location parameter Set

$$\begin{aligned} \frac{\partial Q(\theta, \theta^{(m-1)})}{\partial \mu_k} &= \frac{\nu_k^{(m-1)}}{(\sigma_k^{(m-1)})^{\nu_k^{(m-1)}}} \left(\sum_{x_n \geq \mu_k^{(m-1)}} z_{kn}^{(m-1)} (x_n - \mu_k^{(m-1)})^{\nu_k^{(m-1)} - 1} \right. \\ &\quad \left. - \sum_{x_n < \mu_k^{(m-1)}} z_{kn}^{(m-1)} (\mu_k^{(m-1)} - x_n)^{\nu_k^{(m-1)} - 1} \right) = 0. \end{aligned} \quad (8)$$

Since equation 8 is non-linear, the iterative Newton-Raphson method is applied as follows:

$$\mu_k^{(m)} = \mu_k^{(m-1)} - \frac{g(\mu_k^{(m-1)})}{g'(\mu_k^{(m-1)})}, \quad (9)$$

where $g(\mu_k^{(m-1)})$ is the $Q(\theta, \theta^{(m-1)})$ first order derivative with respect to μ_k , while $g'(\mu_k^{(m-1)})$ is the second order derivative. A detailed version of equation 9 is derived in Appendix C.

Scale parameter Set

$$\begin{aligned} \frac{\partial Q(\theta, \theta^{(m-1)})}{\partial \sigma_k} &= \sum_{n=1}^N z_{kn}^{(m-1)} \left(-\frac{1}{\sigma_k^{(m-1)}} \right) + \frac{\nu_k^{(m-1)}}{(\sigma_k^{(m-1)})^{\nu_k^{(m-1)} + 1}} \\ &\quad \times \sum_{n=1}^N z_{kn}^{(m-1)} |x_n - \mu_k^{(m-1)}|^{\nu_k^{(m-1)}} = 0. \end{aligned}$$

after some calculations, it is possible to obtain the following update (Bazi et al., 2006; Wen et al., 2022)

$$\sigma_k^{(m)} = \left[\frac{\nu_k^{(m-1)} \sum_{n=1}^N z_{kn}^{(m-1)} |x_n - \mu_k^{(m-1)}|^{\nu_k^{(m-1)}}}{\sum_{n=1}^N z_{kn}^{(m-1)}} \right]^{\frac{1}{\nu_k^{(m-1)}}}. \quad (10)$$

Shape parameter As discussed in Section 1, the estimation of the shape parameter within the MLE framework is quite complex presenting the risk of numerical and degeneracy issues. To overcome these issues we introduce an adaptive step size function which depends on the current value of the shape parameter.

Set

$$\begin{aligned} \frac{\partial Q(\theta, \theta^{(m-1)})}{\partial \nu_k} &= \sum_{n=1}^N z_{kn}^{(m-1)} \frac{1}{\nu_k^{(m-1)}} \left(\frac{1}{\nu_k^{(m-1)}} \Psi \left(\frac{1}{\nu_k^{(m-1)}} \right) + 1 \right) \\ &\quad - \sum_{n=1}^N z_{kn}^{(m-1)} \left[\frac{x_n - \mu_k^{(m)}}{\sigma_k^{(m)}} \right]^{\nu_k^{(m-1)}} \log \left[\frac{x_n - \mu_k^{(m)}}{\sigma_k^{(m)}} \right] = 0. \end{aligned} \quad (11)$$

Since the above equation is a non-linear equation, the iterative Newton-Raphson method is applied as follows:

$$\nu_k^{(m)} = \nu_k^{(m-1)} - \alpha(\nu^{(m-1)}) \frac{g(\nu_k^{(m-1)})}{g'(\nu_k^{(m-1)})}, \quad (12)$$

where $g(\nu_k^{(m-1)})$ is the first-order derivative of $Q(\theta, \theta^{(m-1)})$ with respect to ν_k , $g'(\nu_k^{(m-1)})$ is the second-order derivative and

$$\alpha(\nu^{(m-1)}) = e^{-\nu_k^{(m-1)}} \quad (13)$$

represents the proposed adaptive step size function. The function is conceived to avoid the degeneracy of the shape parameter since the magnitude of the Newton step reduces as $\nu_k^{(m-1)}$ increases.

The standard updating equation of the *plain* ECM algorithm (Bazi et al., 2006; Wen et al., 2022) can be recovered by setting $\alpha(\nu^{(m-1)}) = 1$. A more detailed derivation of equation 12 is provided in Appendix C.

Stopping criterion In the motivating example of Section 1 it has been noticed that maximizing the likelihood when updating the shape parameter may lead to spurious solutions. To mitigate this issue, we propose to assess the convergence of the shape parameter by monitoring the first derivative of the Q function with respect to ν_k and not to update the shape parameter when $g(\nu_k)$ is less than a given constant η . The idea is that $g(\nu_k) < \eta$ could be evidence that the likelihood surface is flat with respect to the shape parameter (see Figure 3). In this circumstance, the iterative update of ν such that the likelihood value increases may lead to a spurious solution. As a backup check, the convergence of the location and scale parameters is evaluated following the standard EM stopping criterion based on the difference in the likelihood value. However, from the simulation study it turned out that once $g(\nu_k) < \eta$, the mixing proportions, the mean and the scale parameters have already converged showing that the shape parameters are the last to stabilise.

4 Simulations

The main objective of this section is to study the performance of the proposed ECMs algorithm. By comparing across different simulated scenarios the ECMs results with those

obtained using the *plain* ECM algorithm, we can investigate the benefits of the introduced innovations, *i.e.* the adaptive step size function and the modified stopping criterion. The simulated scenarios are shown in Table 2. Scenario 1 shares the parameter setting of the motivating example. In Scenario 2, the overlap between the two components of the mixture increases by imposing common location parameters ($\mu_1 = \mu_2 = 0$), while the scale parameters are switched between the components compared to scenario 1. Scenarios 3 and 4 feature a normally distributed main component ($\nu_1 = 2$) and a less frequent component with heavy tails ($\nu_2 = 0.8 < 1$). In Scenario 4, the mixture components have common location parameters.

Table 2: MGND simulated scenarios

	π_1	μ_1	σ_1	ν_1	π_2	μ_2	σ_2	ν_2
Scenario 1	0.7	1	3	5	0.3	5	1	1.5
Scenario 2	0.7	0	1	5	0.3	0	3	1.5
Scenario 3	0.7	1	1	2	0.3	5	3	0.8
Scenario 4	0.7	0	1	2	0.3	0	3	0.8

For each scenario, $S = 250$ samples are generated with the composition method (Rizzo, 2019) described in Algorithm 3 (Appendix D) with size $N = 250, 1000$. In each sample, we run the ECM and ECMs algorithms using the same 10 starting points as described in the Appendix D. As measures of quality estimation, the average of the estimates (AVG) and the root mean square error (RMSE) are computed for each parameter as follows:

$$\text{AVG}_\theta = \frac{1}{S} \sum_{s=1}^S \hat{\theta}_s. \quad (14)$$

and

$$\text{RMSE}_\theta = \sqrt{\frac{1}{S} \sum_{s=1}^S (\hat{\theta}_s - \theta)^2}, \quad (15)$$

where θ is the true parameter value and $\hat{\theta}_s$ is the estimate of θ for the s -th simulated data.

Tables 5 and 6 (Appendix E) report all the simulation results. Figure 5 presents the box plot estimates of the shape parameters in Scenario 1 where the true values of ν_1 and ν_2 are 5 and 1.5, respectively.

The results confirm the conclusions drawn in the motivating example in Section 1. Looking at the left panel of figure 5, it is evident that, when the sample size is small, the ECM algorithm suffers a degeneracy problem providing several spurious solutions characterised by very large estimates of the shape parameter ν_1 . On the other hand, the proposed ECMs algorithm largely manages to prevent the degeneracy issue. For $N = 250$, estimates obtained with the ECM algorithm result in $\text{RMSE}_{\nu_1} = 2.99$ compared to $\text{RMSE}_{\nu_1} = 1.47$ of the algorithm ECMs (Scenario 1 results of Table 5). The proposed ECMs algorithm provides more accurate estimates of the other parameters that reduce, for example, the RMSE of ν_2 from

1.96 to 1.28. For large samples ($N = 1000$), the proposed ECMs algorithm is still able to improve on ECM by reducing the RMSE for all parameters. The reduction in RMSE is on the order of 27% and 51% in the estimation of ν_1 and ν_2 and of around 45% in the estimation of the mean parameters. Interestingly enough, RMSE reductions are observed also for the estimation of the scale parameters, even if the updates in the two algorithms coincide. In fact, being the ECM characterised by conditional maximization steps, poor parameter updates of μ_k and ν_k will of course affect the update of the scale parameter σ_k .

Degeneracy issues are also observed in scenario 2 when $N = 250$ where RMSE_{ν_1} equal to 56.65 for ECM. The issue is solved by the ECMs algorithm where $\text{RMSE}_{\nu_1} = 1.35$. Unlike Scenario 1, for large sample sizes ($N = 1000$) the degeneracy problem disappears and the accuracies of ECM and ECMs are similar.

As expected, the ECM algorithm does not report any degeneracy problem in Scenario 3 and 4 since the true shape parameter values are not greater than 2. Generally, in these scenarios, similar estimation results are obtained for the mean and scale parameters, while slightly more accurate parameter estimates are obtained for the shape parameter when the ECMs algorithm is used (Table 6).

Further simulation results are reported in the supplementary materials with the same 4 scenarios but with switched mixing proportions, *i.e.* $\pi_1 = 0.3$ and $\pi_2 = 0.7$. The higher weight in the second component, characterised by larger variability, has the effect of increasing the components overlap. Again, ECM algorithm suffers from degeneracy issues and notable ECMs RMSE gains are spotted for all parameters in the first two scenarios. However, with reversed proportions, the results obtained by ECM and ECMs within scenarios 3 and 4 are no longer similar to each other. Instead, an overall better performance of ECMs is detected for all parameters and sample sizes. In summary, the proposed ECMs algorithm either provides more accurate parameter estimates compared to the ECM algorithm when the shape parameter is greater than 2, the sample size is low and the components overlap is high or returns similar results in the remaining scenarios.

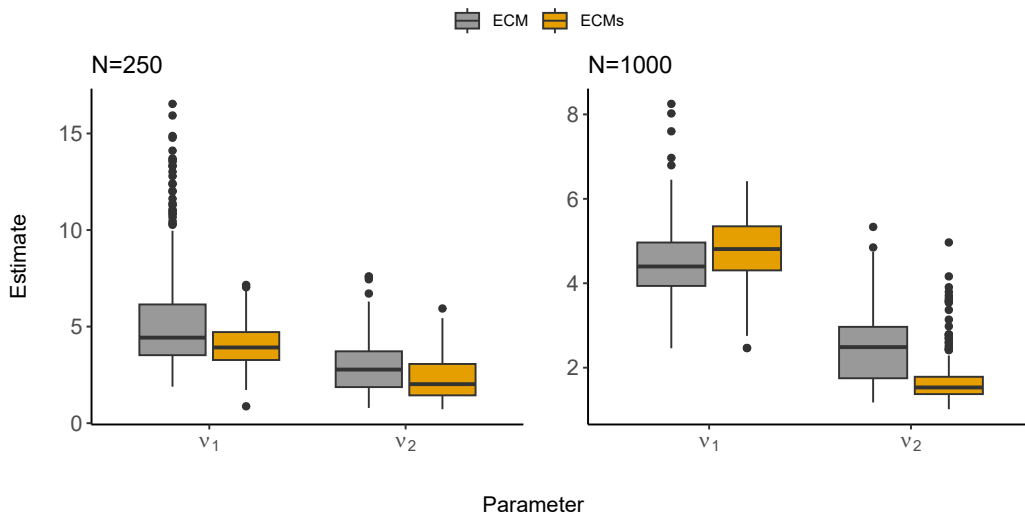


Figure 5: Boxplot of shape parameter estimates for Scenario 1 with $\nu_1 = 5$ and $\nu_2 = 1.5$.

5 Real data analysis

This section presents an analysis of the Euro Stoxx 50 (SX5E) index over the period 2010-2024. Log-returns are computed, and their distribution is analysed with the MGND, mixture of normals (MND) and mixture of student-t distributions (MSTD). The models' performance is assessed using the Akaike Information Criterion (AIC) and Bayesian Information Criterion (BIC). The comparison is also extended to the 50 constituent stocks of the SX5E.

5.1 Euro stoxx 50

Data on daily closing prices of the SX5E have been collected from Yahoo Finance (2024) for the time period January 4, 2010 to September 30, 2024 (3786 observations). The return r_t at time t is defined as follows

$$r_t = (\log P_t - \log P_{t-1})100, \quad (16)$$

where P_t and P_{t-1} are the closing prices at time t and $t - 1$, respectively.

Figure 6 shows the time series where two important volatility periods can be observed: the global financial crisis (2007-2008) and the Covid-19 crisis (2020-2021). The daily returns of the SX5E are not normally distributed because they are characterised by heavy tails, leptokurtosis, and negative skewness (Duttalo et al., 2021) as shown in table 3.

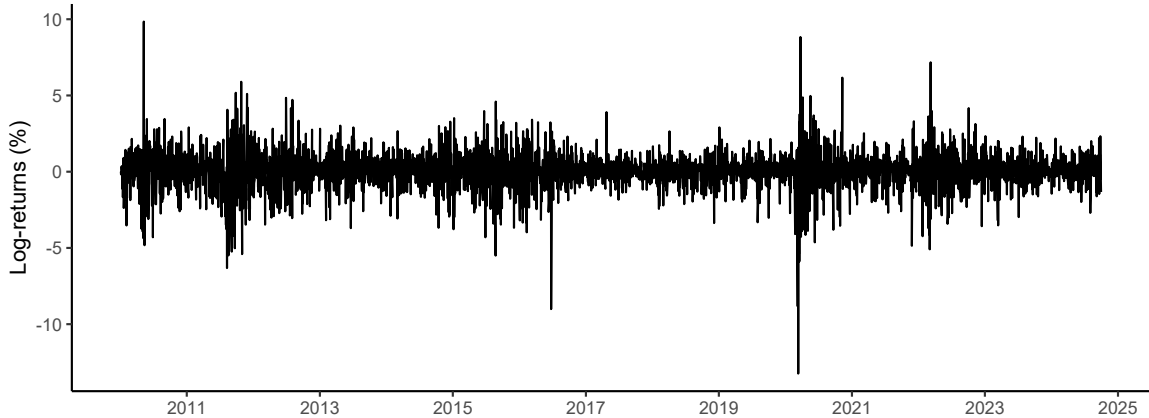


Figure 6: Daily returns of the SX5E.

Table 3: Descriptive statistic summary.

	Mean	Median	Std	Skew	Kur	JB Test
SX5E	0.013	0.042	1.265	-0.466	11.0513	10377*

Notes. * indicates a p -value ≤ 0.05 .

The goodness-of-fit of the two-component MGND model is compared to that of the two-component mixture of normals (MND) and the two-component mixture of Student-t

distributions (MSTD). The two-component MGND model is estimated using the proposed algorithm ECMs, while MND and MSTD are estimated with the R package *teigen* (Andrews et al., 2011, 2018). All algorithms employ 5 starting points with k-means initialization.

Two goodness-of-fit measures are used to find the best-fit model. The Akaike information criterion (AIC) introduced by Akaike (1974) and defined by

$$\text{AIC} = 2p - 2 \log L(\hat{\theta}), \quad (17)$$

where p is the number of parameters of the model and $\log L(\hat{\theta})$ is the computed log-likelihood. The Bayesian information criterion (BIC) introduced by Schwarz (1978) and defined by

$$\text{BIC} = p \log(N) - 2 \log L(\hat{\theta}), \quad (18)$$

where N is the number of observations. Both AIC and BIC balance the goodness-of-fit with model complexity.

The estimation results are reported in Table 4. The best model is the two-component MGND achieving the lowest AIC and BIC values. The MGND model exhibits bimodal asymmetry, with $\mu_1 < \mu_2$. The first component effectively captures extreme market movements through a low shape parameter, $\hat{\nu}_1 = 0.88841$, while the second component is characterised by a shape parameter of $\hat{\nu}_2 = 1.2106$, which lies between the normal and Laplace distributions (Duttilo et al., 2023).

Figure 7 shows the estimated densities of the SX5E. The estimated densities of the MGND and MSTD models are pretty close.

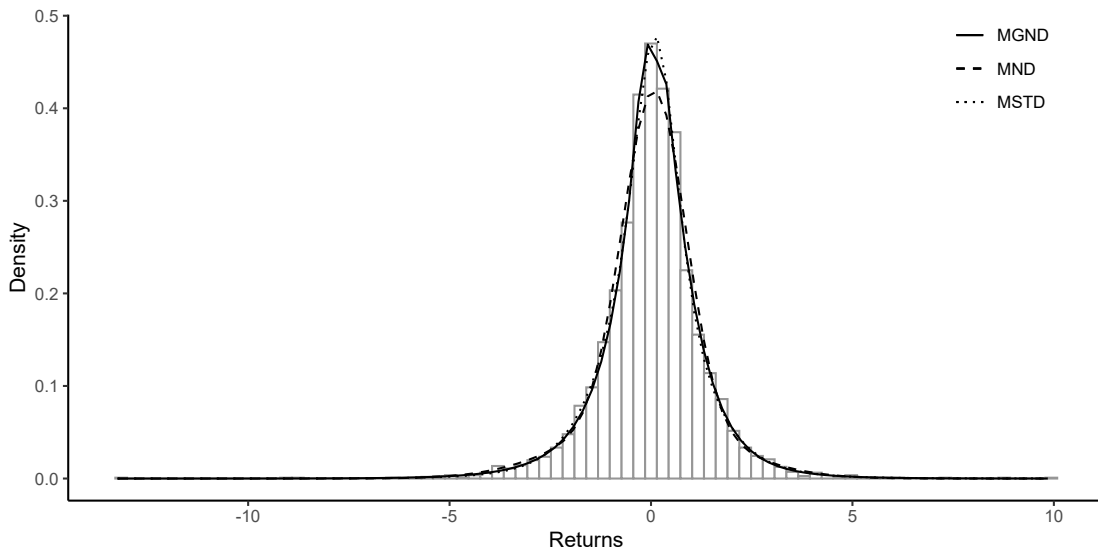


Figure 7: Estimated densities for the SX5E.

Table 4: Estimation results for the SX5E.

	MGND	MND	MSTD
π_1	0.5810	0.7039	0.7220
μ_1	-0.1779	0.0793	-0.0058
σ_1	0.8125	1.1025	1.2262
ν_1	0.8881	-	4.8312
π_2	0.4190	0.2961	0.2780
μ_2	0.3200	-0.1334	0.1239
σ_2	0.8181	2.7725	0.2206
ν_2	1.2106	-	22.6253
$\log L(\hat{\theta})$	-5884.35	-5929.65	-5885.00
AIC	15058.48	15250.81	15063.88
BIC	15104.49	15283.67	15109.89

Notes. In bold the best model according to the goodness-of-fit measures.

5.2 Comparative analysis on Euro stoxx 50 constituents

Data on the daily closing prices of the 50 constituents of the SX5E index have been collected from Yahoo Finance (2024) for the period from January 4, 2010, to September 30, 2024. Daily log-returns for each stock are computed according to equation 16.

Descriptive statistics and the JB test are reported in Table 7 - Appendix E. All stocks exhibit a mean and median close to zero. The standard deviation ranges from 1.2370 to 3.1286. Returns are predominantly negatively skewed, with an empirical kurtosis exceeding three, indicating fat-tailed distributions. The JB test rejects the null hypothesis of normality for all stocks.

Tables 8 and 9 in Appendix E report the AIC and BIC values obtained by MGND, MND and MSTD. The AIC equally selects the MGND and MSTD models in 50% of cases, while the BIC selects the MGND in 50%, the MND in 2%, and the MSTD in 48% of cases. The MGND emerges as a competitive model compared to the MSTD, which is commonly used to fit return distributions (Massing and Ramos, 2021).

6 Conclusions

The main goal of this paper is to provide a satisfactory algorithm that solves the numerical problem of MLE under a mixture model of generalized normals. Indeed, with generalized normal distributions as the subpopulation distributions, the shape parameter M-step of the EM algorithm does not have an analytical solution. The Newton-Raphson update may be used to solve the maximization problem which however may encounter numerical and degeneracy issues which lead to spurious solutions. By introducing an adaptive step size function and by modifying the EM stopping criterion, we aim at avoiding such spurious solutions.

The simulation results have shown that these novelties enhance the accuracy and convergence properties of parameter estimation in MGND models, particularly in scenarios with high shape parameter values, high components overlap and low sample sizes. In addition, the MGND model is applied to the daily returns of the Euro stoxx 50 and its constituents. Comparison with a two-component mixture of normals (MND) and Student-t distributions (MSTD) revealed that the MGND model exhibited superior goodness of fit performance. The MGND model effectively captured the heavy-tailed, leptokurtic and asymmetric properties of the stocks considered, highlighting its potential to model financial time-series data. In conclusion, our study contributes to the advancement of parameter estimation of MGND models, enhancing the accuracy, reliability, and interpretability of the results.

References

- Akaike, H. (1974). A new look at the statistical model identification. *IEEE Transactions on Automatic Control*, 19(6):716–723.
- Allili, M. S., Bouguila, N., and Ziou, D. (2008). Finite general Gaussian mixture modeling and application to image and video foreground segmentation. *Journal of Electronic Imaging*, 17(1):013005.
- Andrews, J. L., McNicholas, P. D., and Subedi, S. (2011). Model-based classification via mixtures of multivariate t-distributions. *Computational Statistics & Data Analysis*, 55(1):520–529.
- Andrews, J. L., Wickins, J. R., Boers, N. M., and McNicholas, P. D. (2018). teigen: An R package for model-based clustering and classification via the multivariate t distribution. *Journal of Statistical Software*, 83(7):1–32.
- Bazi, Y., Bruzzone, L., and Melgani, F. (2006). Image thresholding based on the em algorithm and the generalized gaussian distribution. *Pattern Recognition*, 40(2):619–634.
- Deledalle, C.-A., Parameswaran, S., and Nguyen, T. Q. (2018). Image denoising with generalized gaussian mixture model patch priors. *SIAM Journal on Imaging Sciences*, 11(4):2568–2609.
- Dempster, A. P., Laird, N. M., and Rubin, D. B. (1977). Maximum likelihood from incomplete data via the em algorithm. *Journal of the Royal Statistical Society: Series B (Methodological)*, 39(1):1–22.
- Dutillo, P. (2024). *Modelling financial returns with mixture of generalized normal distributions*. Phd thesis, University "G. d'Annunzio" of Chieti-Pescara, Pescara, IT. Available at https://drive.google.com/file/d/16whH104pVeGu_VY2sN_SPDdbTZeE1jNI/view?usp=sharing.
- Dutillo, P., Gattone, S. A., and Di Battista, T. (2021). Volatility modeling: An overview of equity markets in the euro area during covid-19 pandemic. *Mathematics*, 9(11).

- Dutillo, P., Gattone, S. A., and Iannone, B. (2023). Mixtures of generalized normal distributions and egarch models to analyse returns and volatility of esg and traditional investments. *AStA Adv Stat Anal*, pages 1–33.
- Dytso, A., Bustin, R., Poor, H., and Shamai, S. (2018). Analytical properties of generalized gaussian distributions. *Journal of Statistical Distributions and Applications*, 5(6):1–40.
- Kokkinakis, K. and Nandi, A. K. (2005). Exponent parameter estimation for generalized gaussian probability density functions with application to speech modeling. *Signal Processing*, 85(9):1852–1858.
- Krupiński, R. and Purczyński, J. (2006). Approximated fast estimator for the shape parameter of generalized gaussian distribution. *Signal Processing*, 86(2):205–211.
- Lee, S. X. and McLachlan, G. J. (2013). Model-based clustering and classification with non-normal mixture distributions. *Statistical Methods & Applications*, 22(4):427–454.
- Massing, T. and Ramos, A. (2021). Student’s t mixture models for stock indices. a comparative study. *Physica A: Statistical Mechanics and its Applications*, 580:126143.
- Meng, X.-L. and Rubin, D. B. (1993). Maximum likelihood estimation via the ECM algorithm: A general framework. *Biometrika*, 80(2):267–278.
- Mohamed, O. M. M. and Jaïdane-Saïdane, M. (2009). Generalized gaussian mixture model. In *2009 17th European Signal Processing Conference*, pages 2273–2277.
- Nadarajah, S. (2005). A generalized normal distribution. *Journal of Applied Statistics*, 32(7):685–694.
- Nelder, J. A. and Mead, R. (1965). A Simplex Method for Function Minimization. *The Computer Journal*, 7(4):308–313.
- Nguyen, T. M., Jonathan Wu, Q., and Zhang, H. (2014). Bounded generalized gaussian mixture model. *Pattern Recognition*, 47(9):3132–3142.
- Pogány, T. K. and Nadarajah, S. (2010). On the characteristic function of the generalized normal distribution. *Comptes Rendus Mathematique*, 348(3):203–206.
- Rizzo, M. (2019). *Statistical Computing with R Second Edition (2nd ed.)*. Chapman and Hall.
- Roenko, A. A., Lukin, V. V., Djurovic, I., and Simeunović, M. (2014). Estimation of parameters for generalized gaussian distribution. In *2014 6th International Symposium on Communications, Control and Signal Processing (ISCCSP)*, pages 376–379.
- Schwarz, G. (1978). Estimating the dimension of a model. *The Annals of Statistics*, 6(2):461–464.

Varanasi, M. K. and Aazhang, B. (1989). Parametric generalized Gaussian density estimation. *The Journal of the Acoustical Society of America*, 86(4):1404–1415.

Wen, L., Qiu, Y., Wang, M., Yin, J., and Chen, P. (2022). Numerical characteristics and parameter estimation of finite mixed generalized normal distribution. *Communications in Statistics - Simulation and Computation*, 51(7):3596–3620.

Yahoo Finance (2024). Stock Markets. Accessed: May 28, 2024.

Disclosure statement The authors report that there are no competing interests to declare.

A GND central moments, skewness and kurtosis

The n th central moments of the GDN are obtained as follows

$$E[(X - \mu)^n] = \frac{\sigma^n \{1 + (-1)^n\} \Gamma((n + 1)/\nu)}{2\Gamma(1/\nu)}. \quad (19)$$

Mean, variance, skewness and kurtosis obtained from equation 19 are

$$\begin{aligned} E(X) &= \mu, \\ \text{VAR}(X) &= \frac{\sigma^2 \Gamma(3/\nu)}{\Gamma(1/\nu)}, \\ \text{Sk}(X) &= 0, \\ \text{Kur}(X) &= \frac{\Gamma(1/\nu) \Gamma(5/\nu)}{\Gamma(3/\nu)^2}. \end{aligned} \quad (20)$$

B MGND central moments, skewness and kurtosis

The n th central moments of the MGND model are obtained as follows

$$\begin{aligned} E[X - E(X)]^m &= \sum_{k=1}^K \pi_k \sum_{i=0}^m \binom{m}{i} \left(\mu_k - \sum_{k=1}^K \pi_k \mu_k \right)^{(m-i)} \\ &\times \frac{\sigma_k^i \{1 + (-1)^m\} \Gamma((m + 1)/\nu_k)}{2\Gamma(1/\nu_k)}, \end{aligned} \quad (21)$$

Mean, variance and skewness when $K = 2$ are defined as follows

$$\begin{aligned}
E(X) &= \pi_1\mu_1 + \pi_2\mu_2, \\
\text{VAR}(X) &= \pi_1 \left[\mu_1^2 + \frac{\sigma_1^2\Gamma(3/\nu_1)}{\Gamma(1/\nu_1)} \right] + \pi_2 \left[\mu_2^2 + \frac{\sigma_2^2\Gamma(3/\nu_2)}{\Gamma(1/\nu_2)} \right] + \pi_1\pi_2(\mu_1 - \mu_2)^2, \\
\text{Sk}(X) &= \frac{\pi_1 \left[(\mu_1 - \pi_1\mu_1)^3 + 3(\mu_1 - \pi_1\mu_1) \frac{\sigma_1^2\Gamma(3/\nu_1)}{\Gamma(1/\nu_1)} \right]}{\left[(\mu_1 - \pi_1\mu_1)^2 \frac{\sigma_1^2\Gamma(3/\nu_1)}{\Gamma(1/\nu_1)} \right]^{\frac{3}{2}}} \\
&\quad + \frac{\pi_2 \left[(\mu_2 - \pi_2\mu_2)^3 + 3(\mu_2 - \pi_2\mu_2) \frac{\sigma_2^2\Gamma(3/\nu_2)}{\Gamma(1/\nu_2)} \right]}{\left[(\mu_2 - \pi_2\mu_2)^2 \frac{\sigma_2^2\Gamma(3/\nu_2)}{\Gamma(1/\nu_2)} \right]^{\frac{3}{2}}}, \\
\text{Kur}(X) &= \frac{\pi_1 \left[(\mu_1 - \pi_1\mu_1)^3 + 6(\mu_1 - \pi_1\mu_1)^2 \frac{\sigma_1^2\Gamma(3/\nu_1)}{\Gamma(1/\nu_1)} \frac{\sigma_1^4\Gamma(5/\nu_1)}{\Gamma(1/\nu_1)} \right]}{\left(\left[(\mu_1 - \pi_1\mu_1)^2 + \frac{\sigma_1^2\Gamma(3/\nu_1)}{\Gamma(1/\nu_1)} \right] \right)^2} \\
&\quad + \frac{\pi_2 \left[(\mu_2 - \pi_2\mu_2)^3 + 6(\mu_2 - \pi_2\mu_2)^2 \frac{\sigma_2^2\Gamma(3/\nu_2)}{\Gamma(1/\nu_2)} \frac{\sigma_2^4\Gamma(5/\nu_2)}{\Gamma(1/\nu_2)} \right]}{\left(\left[(\mu_2 - \pi_2\mu_2)^2 + \frac{\sigma_2^2\Gamma(3/\nu_2)}{\Gamma(1/\nu_2)} \right] \right)^2}.
\end{aligned} \tag{22}$$

C Updating equations of the location and shape parameter

Location parameter

$$\mu_k^{(m)} = \mu_k^{(m-1)} - \frac{g(\mu_k^{(m-1)})}{g'(\mu_k^{(m-1)})}, \tag{23}$$

where:

$$\begin{aligned}
g(\mu_k^{(m-1)}) &= \frac{\nu_k^{(m-1)}}{(\sigma_k^{(m-1)})^{\nu_k^{(m-1)}}} \left(\sum_{x_n \geq \mu_k^{(m-1)}} z_{kn}^{(m-1)} (x_n - \mu_k^{(m-1)})^{\nu_k^{(m-1)} - 1} \right. \\
&\quad \left. - \sum_{x_n < \mu_k^{(m-1)}} z_{kn}^{(m-1)} (\mu_k^{(m-1)} - x_n)^{\nu_k^{(m-1)} - 1} \right), \\
g'(\mu_k^{(m-1)}) &= -\frac{\nu_k^{(m-1)}}{(\sigma_k^{(m-1)})^{\nu_k^{(m-1)}}} \left(\sum_{x_n \geq \mu_k^{(m-1)}} z_{kn}^{(m-1)} (x_n - \mu_k^{(m-1)})^{\nu_k^{(m-1)} - 2} \right. \\
&\quad \left. \times (\nu_k^{(m-1)} - 1) + \sum_{x_n < \mu_k^{(m-1)}} z_{kn}^{(m-1)} (\mu_k^{(m-1)} - x_n)^{\nu_k^{(m-1)} - 2} (\nu_k^{(m-1)} - 1) \right).
\end{aligned}$$

After some further calculations, the location parameter of the k -th component is estimated by the following iteration equation (Bazi et al., 2006; Wen et al., 2022)

$$\mu_k^{(m)} = \mu_k^{(m-1)} + \frac{A_k}{B_k} \tag{24}$$

where

$$A_k = \sum_{x_n \geq \mu_k^{(m-1)}}^N z_{kn}^{(m-1)} (x_n - \mu_k^{(m-1)}) \nu_k^{(m-1)-1} - \sum_{x_n < \mu_k}^N z_{kn}^{(m-1)} (\mu_k^{(m-1)} - x_n) \nu_k^{(m-1)-1},$$

$$B_k = \sum_{n=1}^N z_{kn}^{(m-1)} |x_n - \mu_k^{(m-1)}| \nu_k^{(m-1)-2} (\nu_k^{(m-1)} - 1).$$

Shape parameter

$$\nu_k^{(m)} = \nu_k^{(m-1)} - \alpha(\nu_k^{(m-1)}) \frac{g(\nu_k^{(m-1)})}{g'(\nu_k^{(m-1)})}, \quad (25)$$

where:

$$g(\nu_k^{(m-1)}) = \sum_{n=1}^N z_{kn}^{(m-1)} \frac{1}{\nu_k^{(m-1)}} \left(\frac{1}{\nu_k^{(m-1)}} \Psi \left(\frac{1}{\nu_k^{(m-1)}} \right) + 1 \right) - \sum_{n=1}^N z_{kn}^{(m-1)} \left| \frac{x_n - \mu_k^{(m)}}{\sigma_k^{(m)}} \right|^{\nu_k^{(m-1)}} \log \left| \frac{x_n - \mu_k^{(m)}}{\sigma_k^{(m)}} \right|, \quad (26)$$

$$g'(\nu_k^{(m-1)}) = \sum_{n=1}^N z_{kn}^{(m-1)} - \frac{1}{(\nu_k^{(m-1)})^2} \left(1 + \frac{2}{\nu_k^{(m-1)}} \Psi \left(\frac{1}{\nu_k^{(m-1)}} \right) + \frac{1}{(\nu_k^{(m-1)})^2} \Psi' \left(\frac{1}{\nu_k^{(m-1)}} \right) \right) - \sum_{n=1}^N z_{kn}^{(m-1)} \left| \frac{x_n - \mu_k^{(m)}}{\sigma_k^{(m)}} \right|^{\nu_k^{(m-1)}} \times \left(\log \left| \frac{x_n - \mu_k^{(m)}}{\sigma_k^{(m)}} \right| \right)^2.$$

The shape parameter of the k -th component is estimated by the following iteration equation (Bazi et al., 2006; Wen et al., 2022)

$$\nu_k^{(m)} = \nu_k^{(m-1)} - \alpha(\nu_k^{(m-1)}) \frac{\sum_{n=1}^N z_{kn}^{(m-1)} A_k - \sum_{n=1}^N z_{kn}^{(m-1)} B_k}{\sum_{n=1}^N z_{kn}^{(m-1)} C_k - \sum_{n=1}^N z_{kn}^{(m-1)} D_k}, \quad (27)$$

where

$$\alpha(\nu_k^{(m-1)}) = e^{-\nu_k^{(m-1)}}$$

$$A_k = \frac{1}{\nu_k^{(m-1)}} \left(\frac{1}{\nu_k^{(m-1)}} \Psi \left(\frac{1}{\nu_k^{(m-1)}} \right) + 1 \right),$$

$$B_k = \left| \frac{x_n - \mu_k^{(m)}}{\sigma_k^{(m)}} \right|^{\nu_k^{(m-1)}} \log \left| \frac{x_n - \mu_k^{(m)}}{\sigma_k^{(m)}} \right|,$$

$$C_k = -\frac{1}{(\nu_k^{(m-1)})^2} \left(1 + \frac{2}{\nu_k^{(m-1)}} \Psi \left(\frac{1}{\nu_k^{(m-1)}} \right) + \frac{1}{(\nu_k^{(m-1)})^2} \Psi' \left(\frac{1}{\nu_k^{(m-1)}} \right) \right),$$

$$D_k = \left| \frac{x_n - \mu_k^{(m)}}{\sigma_k^{(m)}} \right|^{\nu_k^{(m-1)}} \left(\log \left| \frac{x_n - \mu_k^{(m)}}{\sigma_k^{(m)}} \right| \right)^2,$$

The digamma $\Psi(1/\nu_k)$ and trigamma $\Psi'(1/\nu)$ functions are

$$\Psi(1/\nu_k) = \frac{\partial \Gamma(1/\nu_k)}{\partial(1/\nu_k)} \log \Gamma(1/\nu_k), \quad \Psi'(1/\nu) = \frac{\partial^2 \Gamma(1/\nu_k)}{\partial(1/\nu_k)^2} \log \Gamma(1/\nu_k). \quad (28)$$

D Algorithms

Algorithm 1 MGND model estimation via the ECM algorithm.

1. **require:** data x_1, x_2, \dots, x_N
 2. **set the initial estimates:** k -means initialization minimize $\sum_{k=1}^K W(P_k)$, where P_k denotes the set of units belonging to the k th cluster and $W(P_k)$ is the within cluster deviance

for $k = 1, \dots, K$ **do**

$\mu_k^{(m-1)} \leftarrow \text{mean}(P_k)$, $\sigma_k^{(m-1)} \leftarrow \text{std}(P_k)$, $\nu_k^{(m-1)} \leftarrow$ randomly generated in $[0.5, 3]$,
 $\pi_k^{(m-1)} \leftarrow$ randomly generated in $[0, 1]$, $z_k^{(m-1)} \leftarrow$ Eq. 6

end for

$\log L(\theta^{(m-1)}) \leftarrow$ equation 4, $\epsilon \leftarrow 10^{-5}$
 3. **while** $[\log L(\theta^{(m-1)}) - \log L(\theta^{(m)})] \leq \epsilon$ not convergence **do**

$\mu_k^{(m)} \leftarrow$ Eq. 9, $\sigma_k^{(m)} \leftarrow$ Eq. 10, $\nu_k^{(m)} \leftarrow$ Eq. 12 with $\alpha(\nu^{(m-1)}) = 1$, $\pi_k^{(m)} \leftarrow$ Eq. 7,
 $z_k^{(m)} \leftarrow$ Eq. 6, $\log L(\theta^{(m)}) \leftarrow$ equation 4

evaluate $[\log L(\theta^{(m-1)}) - \log L(\theta^{(m)})] \leq \epsilon$

for $k = 1, \dots, K$ **do**

$\pi_k^{(m-1)} \leftarrow \pi_k^{(m)}$, $\mu_k^{(m-1)} \leftarrow \mu_k^{(m)}$, $\sigma_k^{(m-1)} \leftarrow \sigma_k^{(m)}$, $\nu_k^{(m-1)} \leftarrow \nu_k^{(m)}$

end for

$\log L(\theta^{(m-1)}) \leftarrow \log L(\theta^{(m)})$

end while
 4. **return:** $\theta^{(m)}$, $\log L(\theta^{(m)})$
-

Algorithm 2 MGND model estimation via the ECMs algorithm.

1. **require:** data x_1, x_2, \dots, x_N
 2. **set** $d_k = 0$ for $i = 1, \dots, K$
 3. **set the initial estimates:** k -means initialization minimize $\sum_{k=1}^K W(P_k)$, where P_k denotes the set of units belonging to the k th cluster and $W(P_k)$ is the within cluster deviance
for $k = 1, \dots, K$ **do**
 $\mu_k^{(m-1)} \leftarrow \text{mean}(P_k)$, $\sigma_k^{(m-1)} \leftarrow \text{std}(P_k)$, $\nu_k^{(m-1)} \leftarrow$ randomly generated in $[0.5, 3]$,
 $\pi_k^{(m-1)} \leftarrow$ randomly generated in $[0, 1]$, $z_k^{(m-1)} \leftarrow$ Eq. 6
end for
 $\log L(\theta^{(m-1)}) \leftarrow$ equation 4, $\epsilon \leftarrow 10^{-5}$, $\eta \leftarrow 5^{-3}$
 4. **while** $\left[\log L(\theta^{(m-1)}) - \log L(\theta^{(m)}) \right] \leq \epsilon$ not convergence **do**
for $k = 1, \dots, K$ **do**
 $\mu_k^{(m)} \leftarrow$ Eq. 9, $\sigma_k^{(m)} \leftarrow$ Eq. 10, $g(\nu_k^{(m-1)}) \leftarrow$ Eq. 26
if $g(\nu_k^{(m-1)}) > \eta$ **then** $\nu_k^{(m)} \leftarrow$ Eq. 12 with $\alpha(\nu^{(m-1)}) = e^{-\nu_k^{(m-1)}}$, $d_k \leftarrow 0$ **else** $d_k = 1$
end if
 $\pi_k^{(m)} \leftarrow$ Eq. 7, $z_k^{(m)} \leftarrow$ Eq. 6,
end for
 $\log L(\theta^{(m)}) \leftarrow$ equation 4
if $\sum_{k=1}^K d_k = K$ **then evaluate** $\left[\log L(\theta^{(m-1)}) - \log L(\theta^{(m)}) \right] \leq \epsilon$
end if
for $k = 1, \dots, K$ **do**
 $\pi_k^{(m-1)} \leftarrow \pi_k^{(m)}$, $\mu_k^{(m-1)} \leftarrow \mu_k^{(m)}$, $\sigma_k^{(m-1)} \leftarrow \sigma_k^{(m)}$, $\nu_k^{(m-1)} \leftarrow \nu_k^{(m)}$
end for
 $\log L(\theta^{(m-1)}) \leftarrow \log L(\theta^{(m)})$
end while
 5. **return:** $\theta^{(m)}$, $\log L(\theta^{(m)})$
-

Algorithm 3 Sampling from a MGND with the composition method.

1. **for** $n \in N$ **do**

generate a random u_n from the uniform distribution $U \sim \text{uniform}(0, 1)$

if $\sum_{k=1}^{K-1} \pi_k \leq u_n < \sum_{k=1}^K \pi_k$, generate a random x_n from $f_k(x|\mu_k, \sigma_k, \nu_k)$ using the R function *rgnorm* of the package *gnorm*

2. **return:** simulated data x_1, x_2, \dots, x_N

E Tables

Table 5: MGND simulations, estimated parameters and RMSE.

Scenario 1									
θ	π_1	μ_1	σ_1	ν_1	π_2	μ_2	σ_2	ν_2	N
	0.7	1	3	5	0.3	5	1	1.5	
ECM algorithm									
AVG	0.55	0.45	2.35	5.44	0.45	4.33	1.74	2.94	250
RMSE	0.18	0.87	0.77	2.99	0.18	0.97	0.93	1.96	
AVG	0.58	0.49	2.48	4.51	0.42	4.49	1.66	2.47	1000
RMSE	0.15	0.59	0.59	1.02	0.15	0.60	0.80	1.25	
ECMs algorithm									
AVG	0.60	0.61	2.49	4.05	0.40	4.57	1.45	2.29	250
RMSE	0.17	0.74	0.77	1.47	0.17	0.84	0.82	1.28	
AVG	0.68	0.91	2.88	4.81	0.32	4.91	1.12	1.70	1000
RMSE	0.08	0.34	0.34	0.74	0.08	0.33	0.41	0.61	
Scenario 2									
θ	π_1	μ_1	σ_1	ν_1	π_2	μ_2	σ_2	ν_2	N
	0.7	0	1	5	0.3	0	3	1.5	
ECM algorithm									
AVG	0.67	-0.01	1.18	13.25	0.33	0.02	3.08	1.97	250
RMSE	0.14	0.16	0.89	56.65	0.14	0.36	1.26	1.15	
AVG	0.70	-0.00	1.00	5.07	0.30	0.00	3.05	1.59	1000
RMSE	0.03	0.02	0.03	0.81	0.03	0.17	0.65	0.37	
ECMs algorithm									
AVG	0.72	0.00	0.98	4.19	0.28	0.01	3.43	2.00	250
RMSE	0.06	0.06	0.07	1.35	0.06	0.37	1.19	0.95	
AVG	0.71	-0.00	0.99	4.65	0.29	0.00	3.22	1.67	1000
RMSE	0.03	0.02	0.03	0.71	0.03	0.17	0.63	0.39	

Table 6: MGND simulations, estimated parameters and RMSE.

Scenario 3									
θ	π_1	μ_1	σ_1	ν_1	π_2	μ_2	σ_2	ν_2	N
	0.7	1	1	2	0.3	5	3	0.8	
ECM algorithm									
AVG	0.70	1.00	1.00	2.21	0.30	5.04	3.32	0.87	250
RMSE	0.02	0.06	0.12	0.63	0.02	0.53	1.43	0.24	
AVG	0.70	1.00	1.00	2.06	0.30	5.01	3.22	0.84	1000
RMSE	0.01	0.03	0.05	0.25	0.01	0.25	0.75	0.11	
ECMs algorithm									
AVG	0.70	1.00	0.99	2.15	0.30	4.99	3.33	0.88	250
RMSE	0.02	0.06	0.11	0.53	0.02	0.53	1.50	0.26	
AVG	0.70	1.00	1.00	2.05	0.30	4.99	3.15	0.83	1000
RMSE	0.01	0.03	0.05	0.25	0.01	0.24	0.75	0.10	
Scenario 4									
θ	π_1	μ_1	σ_1	ν_1	π_2	μ_2	σ_2	ν_2	N
	0.7	0	1	2	0.3	0	3	0.8	
ECM algorithm									
AVG	0.73	-0.00	0.99	2.11	0.27	0.04	5.62	1.28	250
RMSE	0.07	0.07	0.12	0.71	0.07	1.00	4.18	1.07	
AVG	0.72	-0.00	1.00	1.99	0.28	0.03	4.22	0.95	1000
RMSE	0.04	0.03	0.06	0.28	0.04	0.36	2.03	0.25	
ECMs algorithm									
AVG	0.73	-0.00	0.99	2.02	0.27	0.04	5.62	1.22	250
RMSE	0.07	0.07	0.12	0.52	0.07	0.98	4.03	0.69	
AVG	0.71	-0.00	1.00	2.01	0.29	0.02	3.93	0.92	1000
RMSE	0.04	0.03	0.06	0.27	0.04	0.37	1.98	0.24	

Table 7: Descriptive statistics of daily log-returns on SX5E constituents.

Tickers	N	Mean	Median	Std	Skewness	Kurtosis	Min	Max	JB
ABI.BE	3786	0.0126	0.0155	1.6258	-0.5261	15.2961	-18.1622	13.4532	24057
AD.NL	3786	0.0319	0.067	1.2615	-0.3433	8.6646	-10.0198	7.7183	5145
ADS.DE	3749	0.0483	0	1.8658	0.2118	11.8965	-16.6886	19.3787	12409
ADYEN.NL	1622	0.0684	0.1629	3.1286	-1.917	50.6746	-49.4034	32.0764	155007
AI.FR	3786	0.0361	0.0551	1.3019	-0.1667	7.7453	-11.8337	8.1161	3576
AIR.FR	3786	0.0587	0.0772	2.1305	-0.3696	16.6907	-25.0623	18.6175	29692
ALV.DE	3749	0.0326	0.069	1.5609	-0.3385	14.1051	-16.6382	14.6728	19362
ASML.NL	3786	0.0902	0.1274	1.9645	-0.0342	6.535	-13.1142	13.0633	1976
BAS.DE	3749	0.0028	0.0496	1.6847	-0.2498	6.7933	-12.5494	10.1917	2291
BAYN.DE	3749	-0.0189	0	1.7967	-0.7681	11.7311	-19.798	9.8678	12294
BBVA.ES	3771	-0.0071	0	2.1928	-0.0765	10.1088	-17.649	19.9073	7956
BMW.DE	3749	0.0235	0.032	1.8212	-0.3276	7.8811	-13.8933	13.5163	3795
BN.FR	3786	0.0109	0.0175	1.237	-0.1645	7.0022	-8.8931	7.4267	2549
BNP.FR	3786	0.0027	0.0407	2.2237	-0.1236	11.1418	-19.1166	18.9768	10482
CS.FR	3786	0.0192	0.0792	1.9485	-0.165	14.6239	-16.8196	19.7782	21360
DB1.DE	3749	0.0359	0.0504	1.5239	-0.4082	9.8567	-12.5985	12.3142	7460
DG.FR	3786	0.0258	0.0498	1.6607	-0.3773	15.9178	-18.7227	17.2666	26448
DHL.DE	3749	0.0259	0.0701	1.5913	-0.2454	7.8797	-12.8063	11.7308	3764
DTE.DE	3749	0.0261	0.0105	1.3685	-0.4423	9.8393	-11.2673	10.6715	7440
EL.FR	3786	0.0432	0.0489	1.4374	0.0345	7.8759	-10.9702	11.1999	3758
ENEL.IT	3748	0.0144	0.0323	1.6522	-0.9864	14.0645	-22.1228	7.6674	19753
ENI.IT	3748	-0.0068	0.0602	1.6936	-1.1388	21.2244	-23.3851	13.9159	52743
IBE.ES	3771	0.0196	0.0444	1.4705	-0.3495	11.6154	-15.1554	13.3703	11756
IFX.DE	3749	0.0531	0.0625	2.2842	-0.2225	6.3665	-17.0262	13.0759	1805
INGA.NL	3786	0.0222	0.0373	2.3247	-0.1945	12.2608	-21.5324	21.9838	13572
ISP.IT	3748	0.0078	0.0565	2.405	-0.6557	12.0401	-26.0594	17.962	13049
ITX.ES	3771	0.0468	0	1.6206	0.2489	7.5087	-11.1276	13.1323	3239
KER.FR	3786	0.0298	0.032	1.846	-0.1225	7.4353	-13.1416	10.0708	3118
MBG.DE	3749	0.0169	0.0391	1.9621	-0.0801	15.3704	-20.8896	24.1193	23940
MC.FR	3786	0.0589	0.0719	1.7051	0.1027	6.251	-9.0777	12.0552	1677
MUV2.DE	3749	0.0405	0.0852	1.4875	-0.2356	21.9209	-19.5309	18.3778	56027
NDA.FI.FI	3695	0.0118	0.0568	1.7814	-0.4705	8.756	-15	12.2009	5246
NOKIA.FI	3695	-0.0248	0.0433	2.4486	-0.7681	20.8655	-26.5878	29.2226	49565
OR.FR	3786	0.0423	0.0422	1.3715	0.1117	6.1634	-7.883	8.1003	1590
PRX.NL	1303	0.0126	-0.0197	2.5987	0.1068	10.5524	-19.015	21.4164	3113
RACE.IT	2235	0.1018	0.1098	1.7443	-0.0381	8.208	-10.8247	10.4542	2534
RI.FR	3786	0.0194	0.035	1.3185	-0.203	6.744	-10.3501	7.5608	2242
RMS.FR	3786	0.083	0.1071	1.5862	-0.0266	8.9923	-12.5081	14.0847	5674
SAF.FR	3786	0.0715	0.0492	1.997	-0.5218	22.6549	-25.9726	19.0064	61187
SAN.ES	3771	-0.0223	0.0174	2.183	-0.2228	12.5898	-22.1724	20.8774	14501
SAN.FR	3786	0.0159	0.0386	1.4176	-1.1407	18.5638	-20.9893	6.2345	39082
SAP.DE	3749	0.0476	0.0783	1.4756	-1.2883	28.0599	-24.7661	11.8219	99254
SGO.FR	3786	0.02	0.0168	1.9277	-0.4681	10.0025	-18.7602	11.2554	7885
SIE.DE	3749	0.0306	0.0484	1.6214	-0.1148	7.906	-13.5774	10.9387	3774
STLAM.IT	3748	0.0447	0.0826	2.5407	-0.4863	7.9363	-19.6792	15.1865	3960
SU.FR	3786	0.0468	0.0877	1.8194	-0.1478	6.9845	-15.1032	11.3445	2523
TTE.FR	3786	0.0085	0.0656	1.6322	-0.5328	15.685	-18.1622	14.0407	25596
UCG.IT	3748	-0.0163	0.0424	2.835	-0.3809	9.7444	-27.1658	19.0067	7205
VOW3.DE	3749	0.0142	0	2.14	-0.501	12.7985	-22.0877	17.434	15176
WKL.NL	3786	0.0606	0.0849	1.2651	-0.427	7.612	-10.2898	7.6426	3476

Table 8: AIC of fitted mixture models for daily log-returns on SX5E constituents.

Ticker	MGND	MND	MSTD
ABI.BE	13447.49	13520.69	13448.94
AD.NL	11820.63	11844.13	11823.79
ADS.DE	14640.47	14678.05	14640.84
ADYEN.NL	7711.15	8286.08	7708.83
AI.FR	12332.44	12355.68	12328.32
AIR.FR	15510.33	15619.72	15513.31
ALV.DE	12937.58	13013.83	12934.18
ASML.NL	15466.69	15495.17	15467.07
BAS.DE	14121.55	14144.35	14121.49
BAYN.DE	14401.87	14491.07	14402.2
BBVA.ES	15985.72	16044.67	15985.89
BMW.DE	14613.6	14654.23	14611.14
BN.FR	11926.2	11945.46	11925.55
BNP.FR	15981.38	16037.3	15984.2
CS.FR	14673.27	14757.34	14669.39
DB1.DE	13232.17	13277.43	13229.01
DG.FR	13653.3	13727.49	13657.08
DHL.DE	13623.83	13661.65	13625.99
DTE.DE	12273.32	12322.28	12269.99
EL.FR	12966.39	12998.84	12963.41
ENEL.IT	13893.14	13980.2	13898.66
ENI.IT	13825.75	13933.24	13817.26
IBE.ES	12824.43	12875.74	12823.73
IFX.DE	16520.46	16554	16522.65
INGA.NL	16171.3	16263.78	16174.22
ISP.IT	16406.79	16488.34	16406.79
ITX.ES	13948.36	13972.2	13947.81
KER.FR	14839.54	14863.58	14842.25
MBG.DE	14961.38	15101.6	14959.13
MC.FR	14391.26	14405.74	14389.41
MUV2.DE	12577.93	12683.63	12574.16
NDA.FI	14121.56	14145.87	14125.39
NOKIA.FI	15791.62	15878.85	15795.86
OR.FR	12777.22	12787.81	12775.61
PRX.NL	5979.8	6001.5	5978.36
RACE.IT	8472.49	8486.66	8481.12
RI.FR	12443.73	12456	12442.96
RMS.FR	13634.53	13672.16	13633.87
SAF.FR	14822.74	14944.58	14822.04
SAN.ES	15987.48	16063.54	15989.82
SAN.FR	12868.76	12918.95	12858.58
SAP.DE	12833.25	12925.96	12826.25
SGO.FR	15146.4	15207.78	15144.97
SIE.DE	13793.46	13815.34	13796.15
STLAM.IT	17117.82	17167.35	17120.35
SU.FR	14854.84	14903.31	14852.85
TTE.FR	13711.88	13799.63	13716.41
UCG.IT	17771.35	17819.32	17773.8
VOW3.DE	15657.64	15776.36	15659.83
WKL.NL	12069.45	12088.58	12070.94

Table 9: BIC of fitted mixture models for daily log-returns on SX5E constituents.

Ticker	MGND	MND	MSTD
ABI.BE	13491.16	13551.88	13492.61
AD.NL	11864.3	11875.33	11867.46
ADS.DE	14684.07	14709.2	14684.45
ADYEN.NL	7748.89	8313.04	7746.57
AI.FR	12376.11	12386.87	12371.99
AIR.FR	15554.01	15650.92	15556.98
ALV.DE	12981.19	13044.98	12977.79
ASML.NL	15510.36	15526.37	15510.74
BAS.DE	14165.16	14175.49	14165.1
BAYN.DE	14445.48	14522.22	14445.8
BBVA.ES	16029.36	16075.84	16029.54
BMW.DE	14657.2	14685.38	14654.74
BN.FR	11969.88	11976.65	11969.22
BNP.FR	16025.05	16068.5	16027.87
CS.FR	14716.94	14788.54	14713.07
DB1.DE	13275.78	13308.58	13272.61
DG.FR	13696.97	13758.69	13700.75
DHL.DE	13667.43	13692.79	13669.59
DTE.DE	12316.92	12353.43	12313.6
EL.FR	13010.06	13030.03	13007.08
ENEL.IT	13936.74	14011.34	13942.26
ENI.IT	13869.35	13964.38	13860.86
IBE.ES	12868.07	12906.91	12867.37
IFX.DE	16564.06	16585.14	16566.25
INGA.NL	16214.97	16294.97	16217.9
ISP.IT	16450.39	16519.48	16450.39
ITX.ES	13992.01	14003.38	13991.45
KER.FR	14883.21	14894.78	14885.92
MBG.DE	15004.98	15132.75	15002.74
MC.FR	14434.94	14436.93	14433.08
MUV2.DE	12621.53	12714.78	12617.77
NDA.FI	14165.06	14176.95	14168.89
NOKIA.FI	15835.12	15909.93	15839.37
OR.FR	12820.89	12819.01	12819.28
PRX.NL	6016	6027.36	6014.57
RACE.IT	8512.47	8515.22	8521.1
RI.FR	12487.4	12487.2	12486.63
RMS.FR	13678.21	13703.36	13677.54
SAF.FR	14866.41	14975.77	14865.72
SAN.ES	16031.13	16094.71	16033.46
SAN.FR	12912.43	12950.15	12902.25
SAP.DE	12876.85	12957.1	12869.86
SGO.FR	15190.07	15238.98	15188.64
SIE.DE	13837.07	13846.49	13839.76
STLAM.IT	17161.42	17198.49	17163.95
SU.FR	14898.52	14934.51	14896.53
TTE.FR	13755.56	13830.82	13760.08
UCG.IT	17814.96	17850.47	17817.4
VOW3.DE	15701.25	15807.51	15703.43
WKL.NL	12113.12	12119.77	12114.61